Monte Carlo Simulations of the Effective Neutron Dose Received by a Male Anthropomorphic Voxel Phantom outside a Medical Linac Treatment Room

M. Hussien, A. K. Ma and N. M. Spyrou
Department of Physics, University of Surrey, Guildford, Surrey, GU2 7XH

Abstract

The effective dose received by an anthropomorphic male phantom outside a medical linear accelerator (Linac) treatment room has been simulated using MCNPX [1]. In high energy Linacs used for electron and photon therapy, unwanted neutrons are produced in the accelerator head which need to be taken into account with regards to inadequate shielding and additional effective dose to staff, primarily. Calculations were made at various positions and orientations outside the room. The highest effective dose due to neutrons was found to be at the maze entrance and the effective dose due to neutron-induced photons was found to contribute an extra 15 % for a person standing facing the maze entrance.

The treatment room was specified so that it could easily be modified; a hospital could provide the dimensions of their Linac treatment room along with specifications such as concrete composition, neutron shielding etc, and simulations could be run to calculate the effective dose in the anthropomorphic phantom to determine whether their shielding is adequate.

Radiotherapy

Radiotherapy is the use of ionising radiations to treat malignant (cancerous) tumours deep within the human body. More than 200 different types of cancer have been identified to date, all cancers however are basically similar; they all result from uncontrolled cell growth causing tumours [2]. External beam therapy is the most common form of radiotherapy and is normally performed with photon beams. These photon beams are generally high energy x-rays produced by a Linac. Modern medical Linacs can produce energies from 8 MeV upto 25 MeV.

Photoneutron production

For descriptive purposes, the energy of neutrons is divided into three energy-ranges [3]:

1.1 Thermal (slow) neutrons: < 0.5 eV
Intermediate neutrons: 0.5 eV – 100 keV
Fast neutrons: >100 keV

The electrons and photons produced in high energy Linacs may undergo electroneutron (e,e'n) interactions and photoneutron (γ,n) interactions respectively. Both types of interactions produce neutrons as by-products [4]. Electroneutron production is 100 times less probable and therefore neglected in simulations. Photoneutron production is governed by the neutron separation energy and by photoneutron cross-sections.

Photoneutron sources include the treatment head, the patient, the air and the walls of the Linac treatment room. So the isotopes of interest include ^{16}O, ^{12}C, ^{14}N, ^{39}K, ^{40}Ca in the patient's body; ^{16}O and ^{14}N in the air; ^{184}W, ^{208}Pb and ^{27}Al in the treatment head and treatment accessories; ^{16}O, ^{28}Si, ^{40}Ca, ^{54}Fe and ^{12}C in the concrete walls. ^{10}B and ^{11}B are sometimes used for maze lining to shield against neutrons.

Linac bunkers are designed to attenuate photons and at the same time moderate the fast photoneutrons produced. The fast neutrons can become thermalized and subsequently captured which results in unwanted radiation.
The photoneutrons produced can result in unwanted dose to not only the patient inside the Linac treatment room but also to oncology staff and the general public outside the treatment room.

Radiation protection governing bodies recommend that a member of the general public and radiation workers should not receive more than 1 mSv and 20 mSv effective dose per year respectively.

Dose Quantities

Absorbed Dose, D, is the energy imparted by ionising radiation to matter per unit mass at a point given in units of J kg^{-1} (commonly called the Gray, Gy) [5]:

$$D = \frac{dE}{dm} \tag{1}$$

The effective dose, E, which is a summation of differing risks to organs in the human body in units of Sieverts (Sv), is given by [6]:

$$E = \sum_T w_T H_T \tag{2}$$

Where w_T is the tissue-weighting factor (Table 1) and HT is the equivalent dose (in Sv) in tissue or organ, T, and is given by [6]:

$$H_T = \sum_R w_R D_{T,R} \tag{3}$$

Where w_R is the radiation weighting factor due to radiation of type R (for example neutron, alpha etc.) and $D_{T,R}$ is the absorbed dose averaged over a tissue or organ, T, due to a radiation of type R.

Table 1. ICRP 1991 and ICRP 2005 proposed tissue-weighting factors. Changes are in bold [7].

ICRP 1991		ICRP 2005 Draft Report	
Tissue or organ	Tissue weighting factor, w_T	Tissue or organ	Tissue weighting factor, w_T
Gonads	**0.20**	Gonads	**0.05**
Bone marrow (red)	0.12	Bone marrow (red)	0.12
Colon	0.12	Colon	0.12
Lung	0.12	Lung	0.12
Stomach	0.12	Stomach	0.12
Bladder	0.05	Bladder	0.05
Breast	**0.05**	**Breast**	**0.12**
Liver	0.05	Liver	0.05
Oesophagus	0.05	Oesophagus	0.05
Thyroid	0.05	Thyroid	0.05
Skin	0.01	Skin	0.01
Bone surface	0.01	Bone surface	0.01
Remainder: adrenals, **brain**, Lower Large Intestine, Upper Large Intestine, **Kidneys**, muscle, pancreas, spleen, thymus, uterus	**0.05**	**Brain**	**0.01**
		Kidneys	**0.01**
		Salivary glands	**0.01**
		Remainder: adipose tissue, adrenals, **connective tissue, extrathoracic airways, gall bladder, heart wall, lymphatic nodes,** muscle, pancreas, **prostate**, small intestine wall, thymus, uterus/cervix	**0.10**

The Anthropomorphic Voxel Phantom

There are two kinds of anatomical body models, mathematical models and voxel (volume pixel) phantoms. Both kinds are referred to as anthropomorphic phantoms, meaning pertaining to human form or attribute. In this project the voxel phantom was used, which can be argued to be more anthropomorphic than the mathematical phantom. The mathematical phantom produced by the Medical Internal Radiation Dose Committee (MIRD) of the Society of Nuclear Medicine [8] has a simple geometrical shape corresponding approximately to the size and shape of the adult human body as far as the major forms and organs are concerned but which neglects minor features. Each organ in the MIRD phantom is considered to be homogeneous in composition and density.

In recent years voxel phantoms have been developed on the basis of tomographic data of real individuals. One of the first voxel phantoms was produced by Zubal et al (1994) [9, 10]. To do this they performed manual segmentation of 129 X-ray Computed Tomography (CT) transverse slices of a healthy adult male and a computerised 3D array modelling all major internal structures was created. Each voxel of the array contains an index number designating it belonging to a given organ or internal structure. This volume array represents a high-resolution model of the human body and has since been used to serve as voxel-based anthropomorphic phantom. Figure 1 shows the clear difference between the mathematical phantom and the anthropomorphic phantom. The phantom used in this project was produced by Alghamdi (2006) [11] at the University of Surrey using tomographic data provided on Zubal's website; see Figure 2

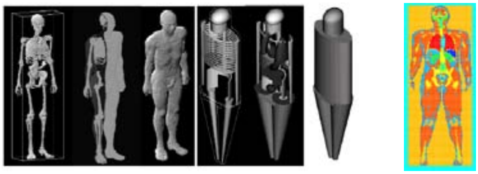

Figure 1. Comparison between the NORMAN voxel phantom (similar to the one used in this project) and ADAM-MIRD mathematical model (Ferrari and Gualdrini, 2005) [12] and Coronal section of the Zubal phantom used in this project, (Alghamdi, 2006) [11]. The phantom comprises millions of voxels.

Linac Shielding Design

To attenuate the high-energy photons, the walls of the Linac bunker are made of thick concrete; in this case 1 m thick. Treatment rooms employ a maze to moderate (slow down) neutrons; in this case a double-bended maze. Some treatment rooms have a single maze, but use a heavy door (weighing roughly 1 ton).

Each wall is 100 cm thick and is assumed to be standard concrete, density ρ = 2.43 g cm^{-3}, with the following percentage composition by weight: 0.99985% ^{1}H, 51.35125% ^{16}O, 1.5% ^{23}Na, 0.2% ^{26}Mg, 2% ^{27}Al, 35% ^{28}Si, 0.15% ^{38}K, 7.284% ^{40}Ca, 0.08% ^{53}Fe, 1.298% ^{55}Fe, 0.032% ^{56}Fe, 0.004% ^{57}Fe, and 0.1009% ^{12}C [13].

The treatment room is assumed to be at ground level and therefore soil is specified beneath the bunker. Soil is assumed to have ρ = 1.25 g cm^{-3} and composition by weight: 16.87% ^{1}H, 27% ^{16}O, 7.5% ^{26}Al, and 48.63% ^{28}Si [4]. Of course the composition for soil is not accurate, as the water content will normally depend on the weather.

Source

The photoneutron spectrum is closely approximated by a ^{252}Cf neutron fission spectrum.

A ^{252}Cf fission source spontaneously emits neutrons and photons. The fission neutron spectrum is described approximately by the following Maxwellian equation [14]:

$$F_n(E_n) = C_n E^{1/2} \exp(-E_n / E_0) \quad (5)$$

where C_n is a constant of 2.31×10^9 neutron mg^{-1} s^{-1} and E_0 is a constant of 1.42 MeV. This spectrum is used as the photoneutron source in the Linac treatment room MCNPX calculations.

Method

MCNPX can be instructed to make tallies related to particle flux and energy deposition. Fluxes across any set of surfaces, surface segments, sum of surfaces, and in cells, cell segments, or sum of cells can be tallied. Heating and fission tallies give the energy deposition in specified cells. In this work all tallies are functions of energy (but it is possible to specify tallies as functions of time) and are normalized to be per starting particle [1].

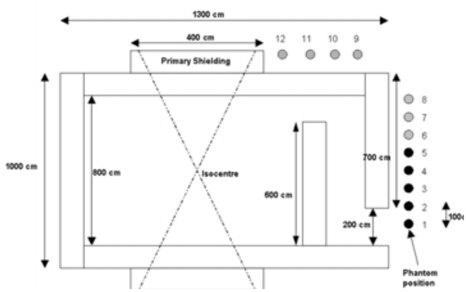

Figure 2. Top-down schematic of the Linac bunker

The ^{252}Cf source was placed at the isocentre of the treatment room. The neutrons were tallied on a surface positioned in 5 different positions (1 – 5) along a line 100 cm from the right hand wall as shown in Figure 2. Simulations were not performed at positions 6 to 8 as they were assumed to be roughly the same as position 5. It was assumed that the control panel (where oncology staff would be standing) would be where positions 1 – 8 are. In the treatment room simulations the photoneutrons are tallied on a surface representing the Anterior-Posterior (phantom facing incoming neutrons) and Posterior-Anterior (phantom with their back to neutrons) plane of the voxel phantom, and separately a surface representing the Right Lateral (RLAT) and Left Lateral (LLAT) planes.

Due to the complexity of integrating the voxel phantom input file into the treatment room input file the simulations to calculate the effective dose were performed in two stages. The neutron fluence was tallied into energy bins between 1×10^{-9} MeV and 20 MeV so that an energy distribution was obtained. This distribution was then used as the source for the anthropomorphic voxel phantom and the absorbed dose in various organs and tissue were simulated.

Neutrons were produced in the fast neutron energy range but were moderated to the thermal neutron energy range by the time they reached the tally surfaces.

The absorbed doses calculated are then used to calculate the effective dose. The value for the effective dose at the end is in units of Sv per neutron as MCNPX tallies are normalized to be per starting particle. This therefore enables calculation of the effective dose received by different Linac machines as different models produce different amounts of photoneutrons depending on their design.

Results and Discussions

ICRP 1991 and ICRP 2005 Draft values were calculated to compare the differences. Table 2 shows values of the effective dose received per Gray of photon for the Varian Clinac 20 [15] linear accelerator operating at 18 MV with neutron shielding surrounding the treatment head.

Table 2. Effective neutron doses for AP and PA irradiations

	AP		PA	
Position	**ICRP 1991** E (μSv Gy^{-1})	**ICRP 2005** E (μSv Gy^{-1})	**ICRP 1991** E (μSv Gy^{-1})	**ICRP 2005** E (μSv Gy^{-1})
1	4.168 ± 0.102	0.736 ± 0.017	2.216 ± 0.054	0.486 ± 0.012
2	2.888 ± 0.057	0.513 ± 0.010	1.582 ± 0.031	0.346 ± 0.007
3	1.187 ± 0.033	0.211 ± 0.006	0.635 ± 0.017	0.138 ± 0.004
4	0.467 ± 0.016	0.082 ± 0.003	0.254 ± 0.009	0.055 ± 0.002
5	0.229 ± 0.005	0.041 ± 0.001	0.127 ± 0.003	0.028 ± 0.001

For the Varian Clinac 20 with neutron shielding surrounding the treatment head, the highest Anterior-Posterior (AP) effective dose was found to be 4.168 ± 0.102 μSv Gy^{-1} using ICRP 1991 and 0.736 ± 0.017 μSv Gy^{-1} using ICRP 2005 at position 1. For Posterior-Anterior (PA) the effective dose was found to drop by a factor of roughly 2. The reason the PA dose is lower than the AP dose is that most organs are near the 'front' of the body and therefore there is less shielding from adipose tissue than from bones.

The value for the effective dose drops, as expected, if a person is standing at **position 5**. Calculations at **position 12** were found to be unreliable as they need to be simulated for a longer time period; these should be investigated in future work. For a Varian Clinac 20 **without** any neutron shielding [15] the effective doses increase by a factor of about 2.

Simulations were also performed to calculate the Left Lateral (LLAT) and Right Lateral (RLAT) effective doses at all positions. It was found that the effective dose at LLAT is about 3.8 times lower than the AP effective dose and the RLAT was 4.8 times lower. The reason behind this is that the radiosensitive organs in the abdomen on the **left** side are better protected against neutrons incident on the RLAT plane by the right arm, but quite importantly by the *liver*. The results for the absorbed dose in different organs support this; about 10% of the total RLAT effective dose contribution is from the liver.

This work shows that it was possible to calculate quite accurately the effective dose received by a person and gain information not possible using practical measurements; it is impossible to practically calculate the effective dose in a real human. Practical dosimetric measurements use neutron detection methods, which of course are not ideal. The values of these types of measurement are given in *ambient dose equivalent* (in Sv) that is an estimate of the effective dose; by assuming that the human body can be represented by a homogeneous tissue equivalent sphere [16]. Previous works have measured (using neutron detection) and calculated (using Monte Carlo) the ambient dose equivalent at the maze entrance, along the maze and inside the treatment room [4, 13, 17, 18]. All values of ambient dose equivalent at the maze entrance were of the order of a μSv Gy^{-1}.

A Linac will operate at about 4 Gy per minute and (for example) a prostate cancer patient will typically receive 60 Gy over a period of 30 days (i.e. 2 Gy per visit). Suppose that 10 patients are treated every day and an oncology nurse works 230 days a year. The worst-case scenario would be if a staff member were standing near the maze entrance at the time of each treatment. In this scenario the total effective dose would about be 19.17 mSv per year according to ICRP 1991 and 3.39 mSv per year according to the ICRP 2005 proposed report; the ICRP recommended limit for workers is 20 mSv per year. But it should also be taken into account that these values do not include effective dose due to photons produced by the Linac treatment head or delayed photons due to activation in the concrete.

The neutron-induced activation at the maze entrance was investigated and it was found that neutron induced *prompt* photons contribute to an extra 15% of the effective dose; MCNP only simulates prompt photons but neglects delayed photons. It was also found that changing the concrete composition to Baryte concrete reduces the effective dose by about 8%.

Conclusions and Future Work

The effective dose received by an anthropomorphic male phantom outside a medical Linac treatment has been simulated using MCNPX. Calculations were made at various positions outside the room. The highest effective dose due to neutrons was found to be at the maze entrance and the effective dose due to neutron-induced photons was found to contribute an extra 15 %. It was possible to calculate the dose received by a particular organ, such as the lung, which can help significantly with radiation protection near a medical Linac.
The treatment room was specified so that it can easily be modified; a hospital could provide the dimensions of their Linac treatment room along with specifications such as concrete composition, neutron shielding etc and simulations could be run to calculate the effective dose in the anthropomorphic phantom to determine whether their shielding is adequate.

A significant point to make in this project is that the simulations were done on a **male** anthropomorphic phantom. According to NHS statistics 9 out of 10 oncology nurses are female. Breast cancer is very common in women (although it is worth pointing out that 1% of breast cancer cases occur in men) and with the proposed increase in the tissue-weighting factor in breast tissue from 0.05 to 0.12 in the ICRP 2005 draft report it is important to develop a female anthropomorphic voxel phantom [19] at the University of Surrey. It may have been possible to estimate the absorbed dose to breasts in the male phantom, but as breast tissue is absent in the male phantom this is not possible.

References
1. J F Briesmeister (Ed) (2000). MCNP – a general Monte Carlo n-particle transport code, Version 4C. Report No. LA-13709-M. Los Alamos, LANL.
2. Cancer Research UK (2005). CancerStats – Incidence – UK.
3. H Kiefer, R Maushart (1972). Radiation Protection Measurement. (Pergamon Press).
4. M P W Chin (1999), Neutron Contamination in a Radiotherapy Maze. (MSc Dissertation: University of Surrey).
5. E L Alpen (1998). Radiation Biophysics 2nd edition. (Academic Press).
6. M J Clark, D T Bartlett, P H Burgess, T M Francis, T O Marshall and F A Fry (1993). Dose quantities for protection against external radiation. Documents of the NRPB 4 (3). (NRPB: Chilton).

7. 2005 recommendations of the International Commission on Radiological Protection. ICRP 2005 (Draft).
8. W S Snyder, M R Ford and G G Warner (1978). Estimates of specific absorbed fractions for photon sources uniformly distributed in various organs of a heterogeneous phantom. Society of Nuclear Medicine.
9. G Zubal et al (1994). Computerised three-dimensional segmented human anatomy. Med Phys, 21, 299–302.
10. G Zubal. The Zubal Phantom, Voxel-Based Anthropomorphic Phantoms. http://noodle.med.yale.edu/zubal/info.htm (last viewed April 2006)
11. A Alghamdi (2006), Voxel-based anthropomorphic phantoms with Monte Carlo simulations in neutron dosimetry. (PhD Thesis: University of Surrey).
12. P Ferrari and G Gualdrini (2005). An Improved MCNP version of the NORMAN voxel phantom for dosimetry studies. Phys Med Bio, 50, 4299–4316.
13. J B Awotwi-Pratt (2003), Neutron Dose Equivalent and Spectra Determination for a Medical Linear Accelerator using Dosimetric and Monte Carlo Methods. (PhD Thesis: University of Surrey).
14. S Endo (1999). Reduction of the gamma-ray component from 252Cf fission neutron source – optimization for biological irradiations and comparison with MCNP code. Phys Med Bio, 44, 1207–1218.
15. R C McCall (1987). Neutron yield of medical electron accelerators. Contributed to the 7th International Congress on International Radiation Protection Association, Sydney, Australia.
16. Determination of Operational Dose Equivalent Quantities for Neutrons (2001). ICRU Report 66.
17. E Carinou, V Kamenopoulo and I E Stamatelatos (1999). Evaluation of neutron dose in the maze of medical electron accelerators. Med Phys, 26, 2520–2525.
18. P H McGinley and E K Butler (1991). Evaluation of neutron dose equivalent levels at the maze entrance of medical accelerator treatment rooms. Med Phys, 18, 279 - 281.
19. R Kramer et al (2004b). All about FAX: a Female Adult voXel phantom for Monte Carlo calculation in radiation protection dosimetry. Phys Med Bio, 49, 5203 – 5216.